

OPTICAL VISIBILITY AND CORE STRUCTURE OF VORTEX FILAMENTS IN A BOSONIC SUPERFLUID

F. Dalfovo^{a*}, *R. N. Bisset*^a, *C. Mordini*^{a,b}, *G. Lamporesi*^{a,b}, *G. Ferrari*^{a,b}

^a *INO–CNR BEC Center and Dipartimento di Fisica, Università di Trento
38123, Trento, Italy*

^b *Trento Institute for Fundamental Physics and Applications, INFN
38123, Trento, Italy*

Received April 6, 2018

Contribution for the JETP special issue in honor of L. P. Pitaevskii's 85th birthday

DOI: 10.1134/S0044451018110019

The Gross–Pitaevskii (GP) equation for a superfluid gas of weakly interacting bosons was derived by L. P. Pitaevskii [1] and E. P. Gross [2] in 1961. A rectilinear quantized vortex is a stationary solution of the GP equation where all particles circulate with the same angular momentum \hbar around a line where the density vanishes; the density recovers its asymptotic value n_0 over a length scale characterized by the healing length ξ , which is determined by n_0 and the strength of the interaction.

Quantized vortices have been extensively studied in superfluid ^4He [3], which is a strongly correlated liquid. The core of the vortex in ^4He is only qualitatively captured by the GP equation and more refined theories are needed to account for the atom-atom interactions and many-body effects [4–7]. A direct comparison between theory and experiment for the structure of the vortex core is not available, and is likely unrealistic, the main reason being that the core size in ^4He is of the same order as the atom size. The only way to observe such a vortex thus consists of looking at its effects on the motion of impurities that may be attached to it [8–11]. While impurities act as tracers for the position of vortex filaments in order to infer their motion on a macroscopic scale, the fine structure of the core remains inaccessible.

Conversely GP theory furnishes a very accurate description of dilute ultracold atomic gases in regimes of temperature and diluteness that are attainable in typical experiments with trapped Bose–Einstein con-

densates (BECs) [12, 13], where quantized vortices are also produced and observed with different techniques [14]. However, no detailed quantitative comparison between theory and experiment for the structure of the vortex core in three-dimensional (3D) condensates has yet been performed. A reason is that the healing length ξ in typical trapped BECs, though much larger than in liquid ^4He , is still smaller than the optical resolution. Another reason is that, when illuminating the atomic cloud with light, the result is the optical density, which is determined by an integral of the density along the imaging axis; thus, a vortex filament has a strong contrast only if it is rectilinear and aligned along the imaging axis. One can overcome the first limitation by switching off the confining potential, letting the condensate freely expand. The vortex core expands as well, at least as fast as the condensate radius [15, 16], so that it can become visible after a reasonable expansion time. However, bending and optical resolution have so far strongly limited the quality of comparisons between theory and experiment for the structure of the vortex core (see Fig. 14.10 in [13]).

In this work, we show how we overcome these limitations in order to optically visualize the vortex filaments with enough accuracy to permit a direct comparison with the predictions of the GP theory. We produce BECs of sodium atoms confined in a cigar-shaped harmonic magnetic trap with trap frequencies $\omega_x/2\pi = 9.3$ Hz and $\omega_\perp/2\pi = 93$ Hz. Each condensate has typically 10^7 atoms, with negligible thermal component, and can contain one or more vortices as a result of the Kibble–Zurek mechanism [17, 18] when cooling the gas across the BEC transition. The trapped BEC has a

* E-mail: franco.dalfovo@unitn.it

radial width on the order of $30 \mu\text{m}$ and an axial width that is 10 times larger. The healing length in the center of the condensate is about $0.2 \mu\text{m}$, smaller than the optical resolution. It is also about two orders of magnitude smaller than the radial width of the condensate, which means that, as far as the density distribution is concerned, a vortex is a thin filament living in a 3D superfluid background with a smoothly varying background density, and the local properties of the vortex core are hence almost unaffected by boundary conditions. However, boundaries are still important for the superfluid velocity field. In fact, the ellipsoidal shape of the condensate causes a preferential alignment of the vortex filament along a radial direction so as to minimize its energy; this significantly reduces the bending of the vortex filaments, while at the same time keeping their local core structure three dimensional. Observations are performed by releasing the atoms from the trap and taking simultaneous absorption images of the full atomic distribution along the radial and axial directions after a sufficiently long expansion in free space.

We use the GP equation to simulate both the in-trap condensate with a vortex and its free expansion. The need to accurately describe the dynamics of the system on both the scale of the healing length ξ and the scale of the width of the entire expanding condensate poses severe computational constraints. With this in mind, we are only able to perform simulations up to values of the chemical potential on the order of $10\hbar\omega_{\perp}$, which are smaller than the experimental values, ranging from about 15 to $30\hbar\omega_{\perp}$. Experiments can also be performed for smaller BECs (i.e., smaller μ), but fluctuations in the density distribution become larger and the signal-to-noise ratio for the visibility of vortices in axial imaging becomes too small. The comparison between theory and experiments hence requires an extrapolation of the GP results to larger μ and this is possible thanks to scaling laws which are valid for large condensates [19–21], in the so-called Thomas–Fermi (TF) approximation. In particular, one can prove that the condensate density is very well approximated by an inverted parabola whose shape is preserved during the expansion upon a rescaling of the radii in time according to $R_x(t) = b_x(t)R_x(0)$ and $R_{\perp}(t) = b_{\perp}(t)R_{\perp}(0)$, where the scaling parameters b_x and b_{\perp} are solutions of coupled differential equations.

In axial imaging, a vortex filament can be observed as faint perturbation in the column density n_{col} , that is, the integral of the density along the imaging axis. By subtracting a fitted TF profile n_{col}^{TF} , we obtain the residual column density δn_{col} in order to enhance the signal of the vortex. We can then extract the depth

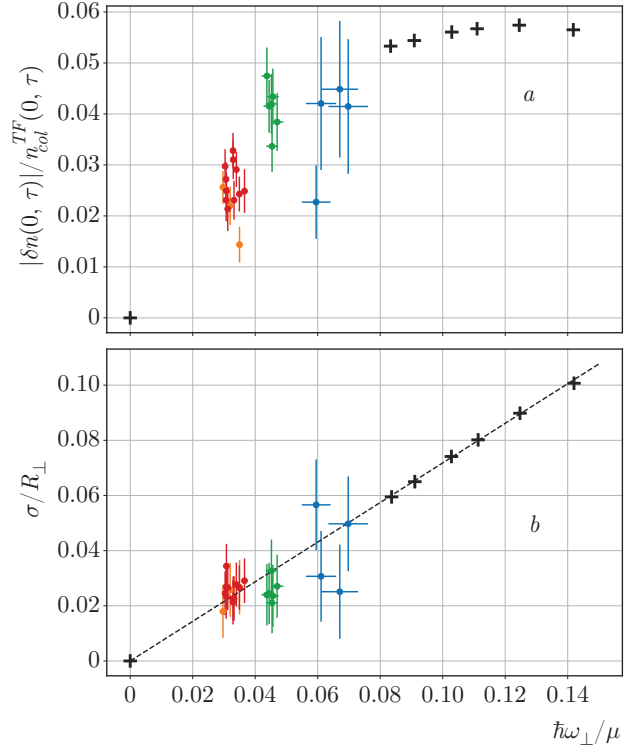


Fig. 1. (Color online) Depth (a) and width (b) of the depletion produced by a vortex in the residual column density for condensates of different μ . The black + symbols are obtained from GP simulations for an expansion time $\tau = \omega_{\perp}t = 70$, corresponding to 120 ms; the point at $1/\mu = 0$ is the limit of an infinitely large condensate, where both quantities must vanish. The dashed line in the panel b is the linear law predicted by GP theory in the TF scaling regime. The colored points with error bars are the different sets of experimental data

and width of the vortex in condensates of different size (i.e., different μ). The same procedure can be applied to the condensates in GP simulations. The results are shown in Fig. 1 as a function of $1/\mu$. The experimental points correspond to four independent sets of data and the error bars account for statistical noise in the residual column density and for the uncertainties in the fit. The GP results clearly show that the rescaled width σ/R_{\perp} scales linearly with $1/\mu$ (dashed line). The figure shows that the experimental data for the width are in good agreement with the GP predictions, especially for the largest condensates, where the vortex signal-to-noise ratio is the largest. For the vortex depth, the GP theory does not provide any simple scaling law; the reason is that the visibility of the vortex in the residual column density exhibits a nontrivial dependence on the expansion time, associated with the crossover from the mean-field dominated early stages of expansion to

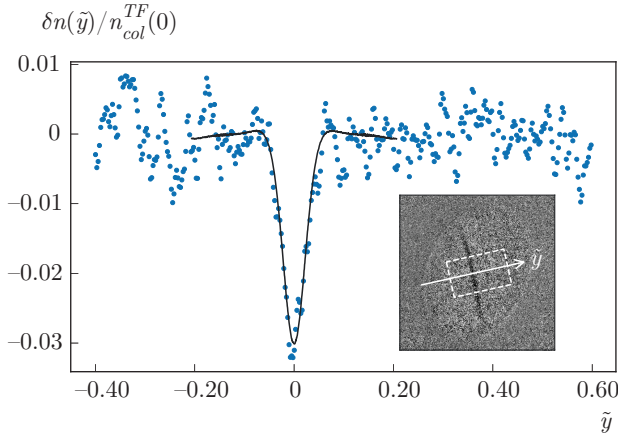


Fig. 2. (Color online) Residual column density after 150 ms of free expansion for a condensate with $2 \cdot 10^7$ atoms and $\mu = 33\hbar\omega_{\perp}$, containing a vortex. The inset shows the full residual column density in the y - z plane. The residual column density is averaged in the direction z within the rectangular box and the resulting values (blue points) are plotted in the main panel as a function of the rescaled coordinate $\tilde{y} = y/R_{\perp}$, where R_{\perp} is the transverse TF radius of the condensate. The solid line is obtained by the same fitting procedure applied to the GP residual column density of a condensate with $\mu = 9.7\hbar\omega_{\perp}$; we linearly rescale its width according to the dashed line of Fig. 1, and reduce its depth to match the experimental value

the later ballistic expansion dynamics. Nevertheless, the experimental points lie in a range fully compatible with a smooth interpolation from the GP results down to the infinite condensate limit.

In Fig. 2, we show an example of vortex profile in a condensate with $2 \cdot 10^7$ atoms and chemical potential $\mu_{\text{expt}} = 33\hbar\omega_{\perp}$, after an expansion time $t = 150$ ms. The full residual column density δn is plotted in the inset. We average this quantity in the z direction within the rectangular box, and the resulting $\delta n(\tilde{y})/n_{\text{col}}^{\text{TF}}(0)$ is shown in the main panel of the figure as a function of \tilde{y} . In order to compare the experimental data with GP theory we proceed as follows. We first check that the shape of the vortex core in the residual column density of GP simulations with different values of μ is the same up to a rescaling of the width and the depth as in Fig. 1, except for small fluctuations in the tails, which are expected to become negligible for large μ . This implies that the GP profile of $\delta n(\tilde{y})/n_{\text{col}}^{\text{TF}}(0)$ for the experimental chemical potential $\mu_{\text{expt}} = 33\hbar\omega_{\perp}$ should be the same as for the GP simulation for $\mu_{\text{GP}} = 9.7\hbar\omega_{\perp}$, after rescaling the width linearly with μ (dashed line in Fig. 1). The solid line in Fig. 2 is the resulting GP profile, where we fixed the depth to the experimental

value. There is good agreement between theory and experiment for the overall shape, including quantitative agreement for the width. The depth has good qualitative agreement if one considers that the experimental value lies within a range between the GP results for smaller μ and the trivial limit for $\mu \rightarrow \infty$, in a way that is compatible with any reasonable smooth interpolation as already shown in Fig. 1a.

In summary, we have shown that quantized vortex filaments can be observed by optical means in three-dimensional atomic BECs, at a level of accuracy which is enough to allow for a direct comparison with the predictions of the Gross-Pitaevskii theory for the width, depth, and overall shape of the vortex core, and we have found good agreement between theory and experiment.

We dedicate this paper to Lev P. Pitaevskii in occasion of his 85th birthday. No words can express our gratitude for the times spent working alongside him and, of course, for his pioneering contributions to physics itself. This work is supported by Provincia Autonoma di Trento and by QuantERA ERA-NET cofund project NAQUAS.

The full text of this paper is published in the English version of JETP.

REFERENCES

1. L. Pitaevskii, Zh. Eksp. Teor. Fiz. **40**, 646 [Sov. Phys. JETP **13**, 451 (1961)].
2. E. P. Gross, Il Nuovo Cimento **20**, 454 (1961).
3. R. J. Donnelly, *Quantized Vortices in Helium II*, Cambridge Univ. Press (1991).
4. F. Dalfovo, Phys. Rev. B **46**, 5482 (1992).
5. G. Ortiz and D. M. Ceperley, Phys. Rev. Lett. **75**, 4642 (1995).
6. S. A. Vitiello, L. Reatto, G. V. Chester, and M. H. Kalos, Phys. Rev. B **54**, 1205 (1996).
7. D. E. Galli, L. Reatto, and M. Rossi, Phys. Rev. B **89**, 224516 (2014).
8. E. J. Yarmchuk, M. J. V. Gordon, and R. E. Packard, Phys. Rev. Lett. **43**, 214 (1979).
9. W. Guo, D. Jin, G. M. Seidel, and H. J. Maris, Phys. Rev. B **79**, 054515 (2009).

10. G. P. Bewley, D. P. Lathrop, and K. R. Sreenivasan, *Nature* **441**, 588 (2006).
11. D. E. Zmeev, F. Pakpour, P. M. Walmsley, A. I. Golov, W. Guo, D. N. McKinsey, G. G. Ihas, P. V. E. McClintock, S. N. Fisher, and W. F. Vinen, *Phys. Rev. Lett.* **110**, 175303 (2013).
12. F. Dalfovo, S. Giorgini, L. P. Pitaevskii, and S. Stringari, *Rev. Mod. Phys.* **71**, 463 (1999).
13. L. Pitaevskii and S. Stringari, *Bose-Einstein Condensation and Superfluidity*, Oxford Univ. Press (2016).
14. A. Fetter, *Rev. Mod. Phys.* **81**, 647 (2009).
15. E. Lundh, C. J. Pethick, and H. Smith, *Phys. Rev. A* **58**, 4816 (1998).
16. F. Dalfovo and M. Modugno, *Phys. Rev. A* **61**, 023605 (2000).
17. G. Lamporesi, S. Donadello, S. Serafini, F. Dalfovo, and G. Ferrari, *Nat. Phys.* **9**, 656 (2013).
18. S. Donadello, S. Serafini, T. Bienaimé, F. Dalfovo, G. Lamporesi, and G. Ferrari, *Phys. Rev. A* **94**, 023628 (2016).
19. Y. Castin and R. Dum, *Phys. Rev. Lett.* **77**, 5315 (1996).
20. Y. Kagan, E. L. Surkov, and G. V. Shlyapnikov, *Phys. Rev. A* **54**, R1753 (1996).
21. F. Dalfovo, C. Minniti, S. Stringari, and L. Pitaevskii, *Phys. Lett. A* **227**, 259 (1997).